

## Ferroelectric phase transition of $\text{Cd}_2\text{Nb}_2\text{O}_7$ studied by Raman scattering

Hiroki Taniguchi,<sup>\*</sup> Takao Shimizu, Hitoshi Kawaji, Tooru Atake, and Mitsuru Itoh  
*Materials and Structure Laboratory, Tokyo Institute of Technology, Yokohama 226-8503, Japan*

Makoto Tachibana

*National Institute for Materials Science, Tsukuba 305-0044, Japan*

(Received 21 November 2007; published 4 June 2008)

Cadmium pyroniobate ( $\text{Cd}_2\text{Nb}_2\text{O}_7$ :CNO) is a recent focus in the ferroelectric materials due to its unusual diffuse-phase transition without any compositional fluctuation, unlike conventional relaxors. In the present study, the critical dynamics of CNO was studied by the confocal micro-Raman scattering. The heavily overdamped soft-mode spectra have been resolved in the ferroelectric phase. The coupled-mode analysis successfully extracted the contribution of the relaxational mode from the overdamped soft mode. The decomposed soft mode clearly shows the Landau-type critical behavior with  $\gamma=1$ . The relaxation was reasonably assigned to the hopping motion of Cd ions from its activation energy of  $\sim 21$  meV. The phase transition of CNO, in spite of diffusive characteristics in the dielectric peak, is concluded to be purely driven by the conventional softening of the soft mode, which is heavily overdamped due to the coupling with Cd-hopping mode.

DOI: [10.1103/PhysRevB.77.224104](https://doi.org/10.1103/PhysRevB.77.224104)

PACS number(s): 77.80.Bh, 77.84.-s, 78.30.-j

Effect of disorder at phase transitions has been a long-standing important issue in condensed-matter physics from both experimental and theoretical viewpoints. Generally, evolution of an order is suppressed and a critical behavior is smeared in a system with defects, impurities, and so on. Ferroelectric counterparts can be seen in doped quantum paraelectrics and relaxors. In  $\text{Sr}_{1-x}\text{Ca}_x\text{TiO}_3$ , a sharp phase transition in the weakly doped system ( $x < 0.011$ ) changes into a rounded one with increasing  $x$ .<sup>1,2</sup> On the other hand, in  $\text{PbMg}_{1/3}\text{Nb}_{2/3}\text{O}_3$ , which is typical relaxor, a frequency-dependent broad dielectric peak is brought about by nanoscopic polar clusters, and macroscopic ferroelectric ordering no longer appears (see Ref. 3 and references therein). These phenomena have generally been explained by a random-field effect due to local electric dipoles, which are induced by the polar impurities. However, in  $\text{Cd}_2\text{Nb}_2\text{O}_7$  (CNO for short), a diffuse-phase transition takes place without any corresponding local polarizations. This feature implies us an uncovered nature of the diffuse-phase transition.

CNO is one of the pyrochlore-type ferroelectric materials, which attracts increasing attention in recent years due to its puzzling phase transition nature.<sup>4-8</sup> It has a complex phase transition sequence, which includes, at least, an improper ferroelastic ( $T_0=205$  K), a proper ferroelectric ( $T_c=196$  K), an incommensurate (85 K), and a commensurate (46 K) phase transitions below room temperature.<sup>4-8</sup> A special attention has been paid to the ferroelectric phase transition around 196 K due to the unusual dielectric response; the relaxorlike broad dielectric peak with strong dispersion and multicomponent relaxation takes place, though the system is, in terms of chemical composition, free from chemical disorder being expected for relaxors in general. Some of the relaxational dynamics were considered to be caused by ferroelectric domains from the results of dielectric measurements under pressure and/or electric field and electric paramagnetic resonance.<sup>9-12</sup> On the other hand, there reported an extra contribution, which was supposed to be the response of Cd ions that form Cd-O zigzag chain, which interpenetrates the corner-connected  $\text{NbO}_6$  network.<sup>5,6,13-15</sup> However, an origin

of diffuse nature and a phase transition mechanism of CNO still remain open questions.

We have preliminary observed a temperature dependence of domain structure across  $T_0$  and  $T_c$ . The domain pattern that was observed just below  $T_c$  is shown in Fig. 1. The [110] and [100] domains, which are related to the improper ferroelastic and proper ferroelectric phase transitions, respectively, coexist in this temperature range. On further cooling, the [100] domains overcome the [110] domains, and finally they take over a whole region of the sample, being in good agreement with previous studies.<sup>5,15,16</sup> We observed the fluctuating domain walls due to the competing two domain structures in the temperature region where the relaxorlike dielectric behavior has been seen. This result suggests that the diffusive characteristic in the ferroelectric phase of CNO is partly caused by the response of unstable ferroelectric domains as suggested by the previous reports.<sup>5,17,18</sup> A focus of present study is to reveal an intrinsic phase transition mechanism of CNO in phonon-frequency region, which is independent of the complex dispersive behavior in the low-frequency region due to the fluctuating domains. If an atomic-scale relaxational process plays an essential role in

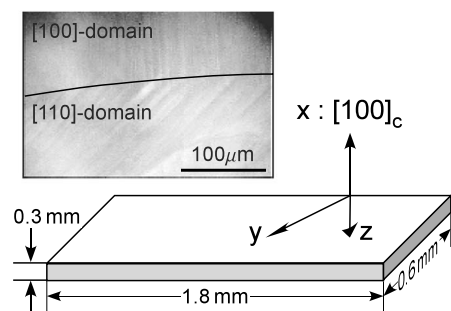


FIG. 1. The sample dimensions and the configurations of the present laboratory coordinate. The picture shows the domain structures at 193 K observed by the crossed nikols polarized-light microscopy.

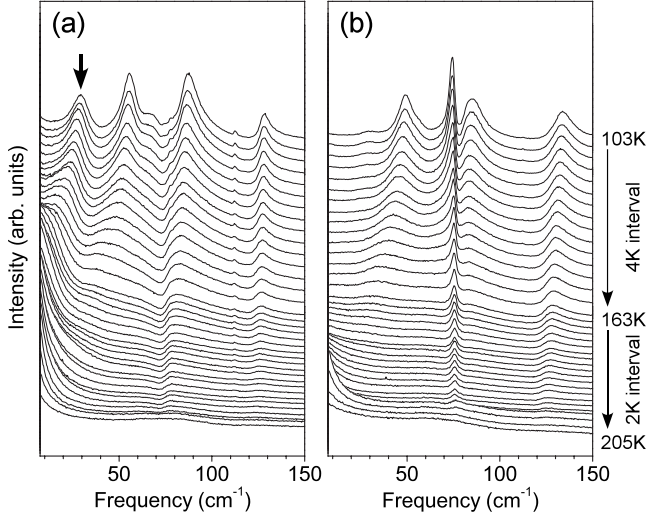


FIG. 2. The temperature dependence of the Raman spectra observed in the (a) scattering geometry and (b)  $\bar{x}(yz)x$  over the temperature range from 103 to 205 K on heating. The phase transition temperature  $T_c=196$  K for the ferroelectric phase transition is pointed by the arrow in the figure. The down arrow in panel (a) indicates the ferroelectric soft mode, which is observed in the present study.

the diffuse-phase transition of CNO, it is expected to be resolved by minute investigations with a light-scattering technique.

In the present study, we performed the confocal micro-Raman experiment on the flux-grown single crystal of CNO, which was cut with the surfaces of (100) and (110) planes and the dimensions of  $1.8 \times 0.6 \times 0.3$  mm<sup>2</sup> (Fig. 1). The wide surfaces were polished into optical quality. An Ar<sup>+</sup> ion laser whose wavelength was 514.5 nm was used for an incident beam with the power of 10 mW on the sample. The incident light was focused into  $\sim 1$   $\mu$ m by the high numerical aperture objective lens on an appropriate region of the sample, which was chosen by a hand-made crossed nikols polarized-light microscopy in order to observe precise light-scattering spectra in an optically homogeneous region. The scattered light, which was polarized by a  $\lambda$  plate, was collected with backscattering geometries,  $\bar{x}(yy)x$  and  $\bar{x}(yz)x$  (laboratory coordinates  $x$ ,  $y$ , and  $z$  are chosen, as denoted in Fig. 1) and analyzed by a triple monochromator Jovin-Yvon T-64000 equipped with a liquid N<sub>2</sub> cooled charge-coupled device camera. A temperature of the sample was controlled by a Linkam THMS600 with the stability of  $<0.1$  K.

Temperature dependencies of the polarized Raman spectra observed in the scattering geometries (a)  $\bar{x}(yy)x$  and (b)  $\bar{x}(yz)x$  are presented in Fig. 2 over the temperature range from 103 to 205 K on heating. The spectral component, which is pointed by the down arrow in Fig. 2(a), is a soft mode that has been observed. On heating, it steeply softens with marked broadening of the spectral shape, seemingly toward 164 K ( $\equiv T_1$ ), which is very far from  $T_c=196$  K. It subsequently becomes a central-peak-like spectral shape above  $T_1$ , indicating its overdamped oscillating nature. This mode vanishes in the  $\bar{x}(yz)x$  scattering geometry, confirming, together with all other spectra, that the present spectra are

taken from the single domain region (or includes only 180-domain region because it does not have any influence on a Raman selection rule). The Raman spectra abruptly lose polarization dependence above  $T_c$ . This feature can be explained by the domain rotation by  $45^\circ$  from [100] to [110] as seen in the polarized microscopy (Fig. 1). Above the lowest-frequency soft mode that was found, another mode, which decreases the frequency on approaching  $T_c$ , was seen around 50 cm<sup>-1</sup> at 103 K. Its temperature dependence is in agreement with the soft mode that was reported in previous Raman studies.<sup>19,20</sup> However, judging from the raw spectra shown in Fig. 2(a), it seems unreasonable to assign it to the soft mode because the softening is incomplete. It is worth mentioning that the lowest soft mode has not been resolved or, exactly speaking, recognized as the central component in the previous spectroscopic studies with Raman or IR techniques, though the upper soft mode was observed. This would be caused by the complicated multidomain state and a strong damping of the soft mode. In the multidomain state, spectra often become ambiguous due to a superposition of differently polarized signals, oblique phonon peaks, and/or multiple scattering at domain walls. In the present study, however, the confocal micro-Raman technique could select the optically homogeneous region, leading to the successful observation of the lowest-frequency soft mode.

In general, an overdamped soft-mode spectrum can be calculated by a damped harmonic-oscillator (DHO) model with a large damping constant. The present spectra, however, could not be reproduced by this method at all, in particular the low-frequency region near 0 cm<sup>-1</sup>, suggesting a contribution of a central component located at zero frequency. Therefore, in order to analyze the low-frequency spectra, we employed a coupled-mode model, which is described by a following dielectric-response function:

$$\epsilon(\omega) = \epsilon(\infty) + \frac{S\omega_{s0}^2}{\omega_{s0}^2 - \omega^2 - \frac{c\omega_{s0}^2}{1-i\omega\tau} - i\omega\Gamma_s}, \quad (1)$$

where  $S$ ,  $\omega_{s0}$ ,  $\Gamma_s$ ,  $\tau$ , and  $c$  represent an amplitude of the coupling mode, a harmonic frequency and a damping constant of the uncoupled soft mode, a relaxation time of the relaxational mode that couples to the soft mode and the coupling constant, respectively.<sup>21-23</sup> The imaginary part of Eq. (1) was used for the calculation in combination with normal DHO functions,

$$I(\omega) \propto \sum_i \frac{A_i \omega_i^2 \Gamma_i \omega}{(\omega_i^2 - \omega^2)^2 + \Gamma_i^2 \omega^2}, \quad (2)$$

where  $A_i$ ,  $\omega_i$ , and  $\Gamma_i$  denotes the amplitude, the frequency, and the damping constant of the  $i$ th mode, respectively.

An example of the fit is shown in Fig. 3(a), where we assumed that only the lowest-frequency mode is coupled to a central peak due to the relaxational mode, but the higher one. There is possibility that the higher softening mode couples with the relaxational mode, since its spectral shape also becomes strongly overdamped near  $T_c$ . Nevertheless, we ignored it for the sake of simplicity. This treatment seems to not so much affect the result because overlapping between the central-peak tail and the higher mode is small. The com-

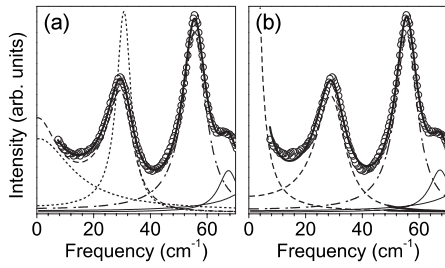


FIG. 3. Spectral calculations by means of (a) the coupled mode described by Eq. (1) with DHOs and (b) the simple combination of the central peak and DHOs. See text for the detail.

bination of the coupled mode and DHOs [solid line in Fig. 3(a)] completely reproduces the spectra of CNO as indicated in the figure. The coupled-mode spectra calculated by Eq. (1) [a broken line in Fig. 3(a)] are composed of two components: the soft-mode spectrum and the central peak [the dotted lines in Fig. 3(a)]. The coupling constant  $c$  was assumed to be independent of temperature with a value of 0.39, which was determined by a least-squares fitting for the spectrum observed at 103 K. A solid line shown in Fig. 3(b) represents, for comparison, a result of the calculation using a simple superposition of the central component and the DHOs without coupling between them. As shown in Fig. 3(b), the fitting is pretty poor in the low-frequency region below  $20 \text{ cm}^{-1}$ . Moreover, the obtained central component is unrealistically large, confirming reasonability of the present analysis.

Temperature dependencies of the calculated soft-mode frequency and half width at half maximum (damping constant) are plotted by closed and open circles in Fig. 4, respectively. Here, according to vibration mechanics for the damped harmonic oscillation, a real frequency of the soft mode  $\omega_s$ , which coincides with intervals between times when the amplitude takes a value of zero, should be given by an equation  $\omega_{\text{soft}} = \sqrt{\omega_{0s}^2 - \Gamma_s^2}$ , with the harmonic frequency  $\omega_{0s}$  and the damping constant  $\Gamma_s$ . Therefore, we plotted  $\omega_s$  as a soft-mode frequency in Fig. 4. As shown in the figure, the soft mode decreases its frequency as the temperature approaches  $T_c$  irrespective of  $T_1$ , at which the soft mode seemingly softens. A solid line was calculated by a Cochran law,  $\omega_s = 3.3|T - 196|^{0.5}$ . The temperature dependence of the soft mode is in excellent agreement with a curve, indicating displacive-type nature of CNO with Landau-type behavior. A broken line is an eye guide for the damping constant, which was calculated by the  $\Gamma_s = 110|T - 196|^{-0.76}$ . Above 183 K ( $\equiv T_2$ ),  $\omega_s$  becomes imaginary ( $\omega_{s,0} < \Gamma$ ). It means the uncoupled soft-mode vibration becomes overdamped above  $T_2$ .  $T_2$  is 13 K below from  $T_c$ , though the raw spectra already become central peaklike at  $T_1$ , which is 32 K below  $T_c$ . Thus, it was revealed that the unusually strong damping of the raw spectra, which makes the soft-mode spectra smeared, is caused by the coupling with the relaxational mode. It should be noted here that some peaks seemingly vanish at  $T_1$ , implying an additional structural phase transition. However, they can be understood as rather heavily damped than vanished. In fact, no change in the domain configuration was detected at  $T_1$  during the polarized microscopy observation, indicating no structural phase transition there.

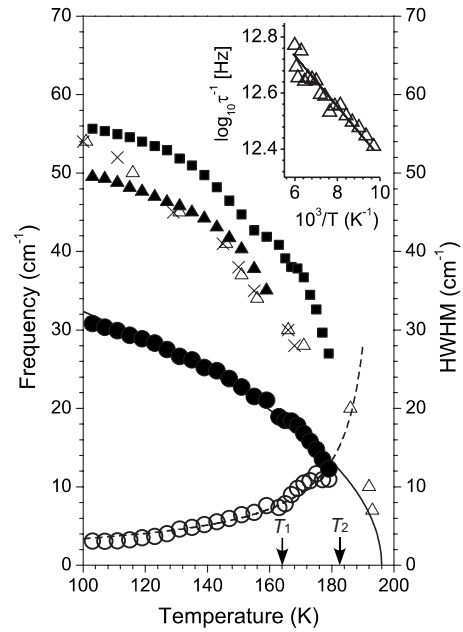


FIG. 4. The temperature dependencies of the frequencies of the lowest-frequency soft mode (solid circles) and the upper softening mode (solid squares). The damping constant of the lower soft mode is plotted by open circles. Closed triangles indicate the temperature dependence of the lowest-frequency mode, which was observed in the  $x(yz)\bar{x}$  scattering geometry. The solid line was calculated by the Cochran law, and the broken line denotes the eye guide for the damping constant (see text for the detail). The soft modes, which were observed in the previous studies, are presented by crosses (Ref. 19) and open triangles (Ref. 20). The inset presents the Arrhenius plot for the relaxation rate, which is obtained from the central component.

The temperature dependence of the frequency of the upper softening mode is plotted by closed squares together with the lowest-frequency mode, which was observed in  $x(yz)\bar{x}$  scattering geometry (closed triangles). The soft modes in the previous studies are presented by open triangles and crosses in comparison.<sup>19,20</sup> All the modes which are located around  $55 \text{ cm}^{-1}$  at 100 K show similar temperature dependences in their frequencies. If the spectra are observed in the multidomain state, two modes, which are plotted by closed triangles and squares, cannot be distinguished and we would identify them as one mode because they are superposed each other due to a loss of Raman selection rule. The soft modes in the previous study possibly observed the superposition of these two modes.

In order to clarify the origin of the relaxational mode that is coupled to the soft mode, we examined the temperature dependence of the relaxational rate by means of Arrhenius plot, as seen in the inset of Fig. 4. The relaxation rate, which was obtained by the calculation, monotonically increases with increasing temperature with a slope, indicating the activation energy of 21 meV. This value roughly coincides with that of an ionic hopping mode, which is previously reported in a ferroelectric perovskite by a first principles calculation.<sup>24</sup> Hence, the origin of the relaxational mode is considered to be the hopping motion of the ions. The previous x-ray study reported the large thermal parameter of the Cd ion.<sup>25</sup> Further-



more, the two-site hopping of the oxygen ions, which form zigzag chain together with Cd ions, was indicated by the electron paramagnetic resonance measurement. Therefore, it is natural to attribute the observed relaxational mode to the dynamics of Cd ions. The phase transition mechanism of CNO, thus, can be explained by the displacive-type phase transition, which is driven by the softening of the soft mode of  $\text{NbO}_6$  octahedral vibrations, which couples to the Cd-hopping mode. The assignment that the soft mode is formed with  $\text{NbO}_6$  octahedra is justified by the dielectric measurement under the pressure, which reported the similarity of the phase transition mechanism between CNO and  $\text{BaTiO}_3$ .<sup>3</sup>

Here, let us summarize the critical dynamics of CNO by comparing the present result with previous ones. The previous Raman and microwave results are basically in agreement with the present result, which concludes the displacive-type second-order phase transition of CNO driven by the conventional Landau-type soft-mode softening.<sup>19,20,26</sup> In contrast, there is a critical discrepancy with the former IR measurement, which suggests that the phase transition of CNO is driven by the relaxational Cd-hopping mode, and its softening is triggered by the coupling with the incomplete soft mode, whose frequency settles with finite value at  $T_c$  on cooling.<sup>5</sup> From the present result, the Cd-hopping mode does not show any critical behavior but obeys Arrhenius law, indicating no active role of Cd-hopping mode in the phase transition of CNO. The role of Cd-hopping mode is considered to enhance the damping of soft mode through the coupling. The inconsistency between the Raman and the IR study would be caused by the difference in resolution for the low-frequency region, since the heavily damped low-frequency mode is generally very difficult to resolve by an IR technique.

Another significant issue in CNO is the coexistence of displacive and order-disorder-type mechanisms suggested by the previous studies, where two dynamics were attributed to the  $\text{NbO}_6$  octahedra-dominated soft mode and Cd-hopping mode.<sup>5,17,27</sup> From the present result, it turned out not to be the case in CNO that the softening of the relaxational mode due to the Cd hopping triggers the crossover between soft-mode-type to order-disorder-type mechanisms. Nevertheless, we cannot rule out the possibility that the crossover between the displacive to the order-disorder-type mechanisms in CNO because the order-disorder-type mechanism has been detected in nominally pure soft-mode systems indeed. In  $\text{BaTiO}_3$ , which was unambiguously concluded to undergo the displacive-type phase transition by a femtosecond time-resolved spectroscopy technique (Refs. 28 and 29), in fact, the order-disorder component was evidenced by several measurements.<sup>30,31</sup> Also in  $\text{PbTiO}_3$  that is textbook displacive-type ferroelectrics, a light-scattering study resolved a contribution of the order-disorder mechanism.<sup>32</sup>

Furthermore, an “intrinsic” order-disorder mechanism in the soft-mode system was suggested by a self-consistent phonon approximation (SCPA) theory on structural phase transition driven by anharmonic lattice vibration (soft mode).<sup>33,34</sup> When we assume Hamiltonian for a system of anharmonic lattice vibrations and analyze the temperature dependence of susceptibility across the phase transition, the result includes order-disorder-type mechanism, though the Hamiltonian is constructed purely based on the soft-mode-type displacive phase transition. According to Refs. 33 and 34, we can examine the order-disorder-type contribution in the soft-mode-type phase transition by using the Rhodes–Wohlfarth plot, which is derived from SCPA. The Rhodes–Wohlfarth ratio  $r(\equiv \mu_c/\mu_s)$  of CNO is around 2 that indicates coexistence of displacive-type mechanism and order-disorder-type one.<sup>35</sup> Here  $\mu_c$  and  $\mu_s$  mean the absolute values of dipole moments that are obtained from Curie constant and spontaneous polarization  $P_s$ . On the other hand, an important indication for the anharmonic lattice vibration system was made by molecular-dynamics studies by Schneider and Stoll.<sup>36,37</sup> They suggested that clusters come out spontaneously and propagate with certain lifetime (so-called polar cluster wave). This implies that dielectric dispersion, which is caused by the response of spontaneous polar clusters, is taken place in the vicinity of  $T_c$  in the displacive-type phase transition. As far as we know, there has been no clear report observing the dispersive characteristics due to spontaneous polar clusters. In CNO, however, the soft mode is strongly anharmonic due to the extra coupling to the Cd-hopping mode; therefore, it is expected that the cluster dynamics would be enhanced strongly. (Probably it takes an essential part in the diffuse-phase transition of CNO.) Unfortunately, the soft-mode theory with strong damping has not been established. It should be conducted for better understanding of the structural phase transition driven by the heavily damped soft mode.

In the present study, the minute temperature dependence of the soft mode in CNO has been resolved by the confocal micro-Raman spectroscopy. The coupled-mode analysis successfully decomposed the soft mode and relaxational mode from heavily overdamped low-frequency spectra. The uncoupled soft mode clearly shows the Landau-type behavior with  $\gamma=1$ , indicating that the phase transition of CNO is purely driven by the soft mode. The coupling relaxational mode does not present any critical behavior but obeys the Arrhenius law with the activation energy of  $\sim 21$  meV that coincides with ionic hopping mode. The Cd-hopping mode was reasonably attributed to the origin of relaxational mode couples to the soft mode.

The present study was supported by a Grant-in-Aid for Scientific Research (A) from JSPS under Grant No. 20246098.

\*taniguchi.h.aa@m.titech.ac.jp

- <sup>1</sup>J. G. Bednorz and K. A. Müller, *Phys. Rev. Lett.* **52**, 2289 (1984).
- <sup>2</sup>U. Bianchi, J. Dec, W. Kleemann, and J. G. Bednorz, *Phys. Rev. B* **51**, 8737 (1995).
- <sup>3</sup>G. A. Samara, *J. Phys.: Condens. Matter* **15**, R367 (2003).
- <sup>4</sup>V. A. Isupov, *Phys. Solid State* **47**, 2119 (2005).
- <sup>5</sup>E. Buixaderas, S. Kamba, J. Petzelt, M. Sanikov, and N. N. Kolpakova, *Eur. Phys. J. B* **19**, 9 (2001).
- <sup>6</sup>G. A. Samara, E. L. Venturini, and L. A. Boatner, *J. Appl. Phys.* **100**, 074112 (2006).
- <sup>7</sup>Z. Yu and C. Ang, *Appl. Phys. Lett.* **85**, 801 (2004).
- <sup>8</sup>M. Tachibana, H. Kawaji, and T. Atake, *Phys. Rev. B* **70**, 064103 (2004).
- <sup>9</sup>C. Ang, J. E. Cross, R. Guo, and A. S. Bhalla, *Appl. Phys. Lett.* **77**, 732 (2000).
- <sup>10</sup>C. Ang, R. Guo, A. S. Bhalla, and J. E. Cross, *J. Appl. Phys.* **87**, 7452 (2000).
- <sup>11</sup>C. Ang, A. S. Bhalla, R. Guo, and J. E. Cross, *J. Appl. Phys.* **90**, 2465 (2001).
- <sup>12</sup>S. Waplak and N. N. Kolpakova, *Phys. Status Solidi A* **117**, 461 (1990).
- <sup>13</sup>N. N. Kolpakova, M. Polomska, and J. Wolak, *Ferroelectrics* **126**, 151 (1992).
- <sup>14</sup>N. N. Kolpakova, R. Margraf, and M. Polomska, *J. Phys.: Condens. Matter* **6**, 2787 (1994).
- <sup>15</sup>N. N. Kolpakova, S. Waplak, and W. Bednarski, *J. Phys.: Condens. Matter* **10**, 9309 (1998).
- <sup>16</sup>Z. G. Ye, N. N. Kolpakova, J.-P. Rivera, and H. Schmid, *Ferroelectrics* **124**, 275 (1991).
- <sup>17</sup>S. Kamba, E. Buixaderas, T. Ostapchuk, and J. Petzelt, *Ferroelectrics* **268**, 163 (2002).
- <sup>18</sup>J. Hlinka, J. Petzelt, S. Kamba, D. Noujni, and T. Ostapchuk, *Phase Transitions* **79**, 41 (2006).
- <sup>19</sup>G. A. Smolensky, N. N. Kolpakova, S. A. Kizhaef, and I. G. Siny, *Ferroelectrics* **44**, 129 (1982).
- <sup>20</sup>N. N. Kolpakova, M. Wiesner, I. L. Shul'pina, and P. P. Symnikov, *Ferroelectrics* **221**, 91 (1999).
- <sup>21</sup>J. A. S. Barker, *Phys. Rev. B* **12**, 4071 (1975).
- <sup>22</sup>J. Toulouse, F. Jiang, O. Svitelskiy, W. Chen, and Z.-G. Ye, *Phys. Rev. B* **72**, 184106 (2005).
- <sup>23</sup>V. L. Ginzburg, A. P. Levanyuk, and A. A. Sobyenin, *Phys. Rep.* **57**, 151 (1980).
- <sup>24</sup>R. Cohen, *Nature (London)* **358**, 136 (1992).
- <sup>25</sup>K. Lukaszewicz, A. Pietraszko, and J. Stepien-Damm, *Mater. Res. Bull.* **29**, 987 (1994).
- <sup>26</sup>J. Banys, J. Grigas, N. N. Kolpakova, R. Sobestijanskas, and E. Sher, *Lith. Phys. J.* **29**, 209 (1989).
- <sup>27</sup>E. Buixaderas, S. Kamba, and J. Petzelt, *Ferroelectrics* **308**, 131 (2004).
- <sup>28</sup>T. P. Dougherty, G. P. Wiederrecht, K. A. Nelson, M. H. Garrett, H. P. Jensen, and C. Warde, *Science* **258**, 770 (1992).
- <sup>29</sup>T. P. Dougherty, G. P. Wiederrecht, K. A. Nelson, M. H. Garrett, H. P. Jenssen, and C. Warde, *Phys. Rev. B* **50**, 8996 (1994).
- <sup>30</sup>B. Zalar, V. V. Laguta, and R. Blinc, *Phys. Rev. Lett.* **90**, 037601 (2003).
- <sup>31</sup>R. Z. Tai, K. Namikawa, A. Sawada, M. Kishimoto, M. Tanaka, P. Lu, K. Nagashima, H. Maruyama, and M. Ando, *Phys. Rev. Lett.* **93**, 087601 (2004).
- <sup>32</sup>M. D. Fontana, H. Idrissi, and K. Wojcik, *Europhys. Lett.* **11**, 419 (1990).
- <sup>33</sup>M. Tokunaga, *J. Phys. Soc. Jpn.* **56**, 1653 (1987).
- <sup>34</sup>M. Tokunaga, *J. Phys. Soc. Jpn.* **57**, 4275 (1988).
- <sup>35</sup>M. Tokunaga, *Physica B* **219&220**, 587(1996).
- <sup>36</sup>T. Schneider and E. Stoll, *Phys. Rev. Lett.* **35**, 296 (1975).
- <sup>37</sup>T. Schneider and E. Stoll, *Phys. Rev. B* **13**, 1216 (1976).